

# A seamlessly coupled GIS and distributed groundwater flow model

Lei Wang\*, Christopher R. Jackson, Magdalena Pachocka, Andrew Kingdon  
British Geological Survey, Keyworth, Nottingham NG12 5GG, UK.

## Highlights

- A seamless GIS-groundwater flow model is presented
- It directly uses GIS data for groundwater flow modelling within the GIS environment
- This easy-to-use and flexible model can be used by non-modellers
- It is downloadable and can be used for any purpose free of charge
- The model developed herein can be integrated into other raster GIS packages.

## Abstract

There are three approaches for coupling groundwater models with GISs, i.e. *loose*, *tight*, and *seamless*. In seamless coupling a model code is written into, and run from within, a GIS. We implemented BGS GISGroundwater in a GIS in this way for the first time. It facilitates the construction and simulation of the model, and the visualisation of the results all within the GIS environment. The model consists of a 2D finite-difference groundwater flow model and a simple user-interface. It can represent heterogeneous aquifers, variably confined and unconfined conditions, and distributed groundwater recharge and abstraction. It offers benefits in terms of ease of use and in streamlining the model construction and application process. BGS GISGroundwater has been validated against analytical solutions to groundwater-head profiles for a range of aquifer configurations. This model lowers barriers to entry to groundwater flow modelling for a wider group of environmental scientists.

Keywords: GIS; Groundwater flow model; Finite-difference method; GISGroundwater

## Software availability

Name of software: BGS GISGroundwater  
Developer: Dr. Lei Wang  
Contact address: British Geological Survey, Environmental Science Centre,  
Keyworth, Nottingham, NG12 5GG, UK.  
Email: lei.wang@bgs.ac.uk

Year first available: 2014  
Software required: ESRI® ArcMap™ 10.0 and above

---

\*Corresponding author: Dr. Lei Wang, British Geological Survey, Environmental Science Centre, Keyworth, Nottingham, NG12 5GG, UK. Phone: +44(0)1159363484. Email: lei.wang@bgs.ac.uk

Program Language: C++

Availability and cost: BGS GISGroundwater can be freely downloaded (with manual and tutorial materials) from <http://www.bgs.ac.uk/GISGroundwater>, and used for any purpose under the Open Government License.

29

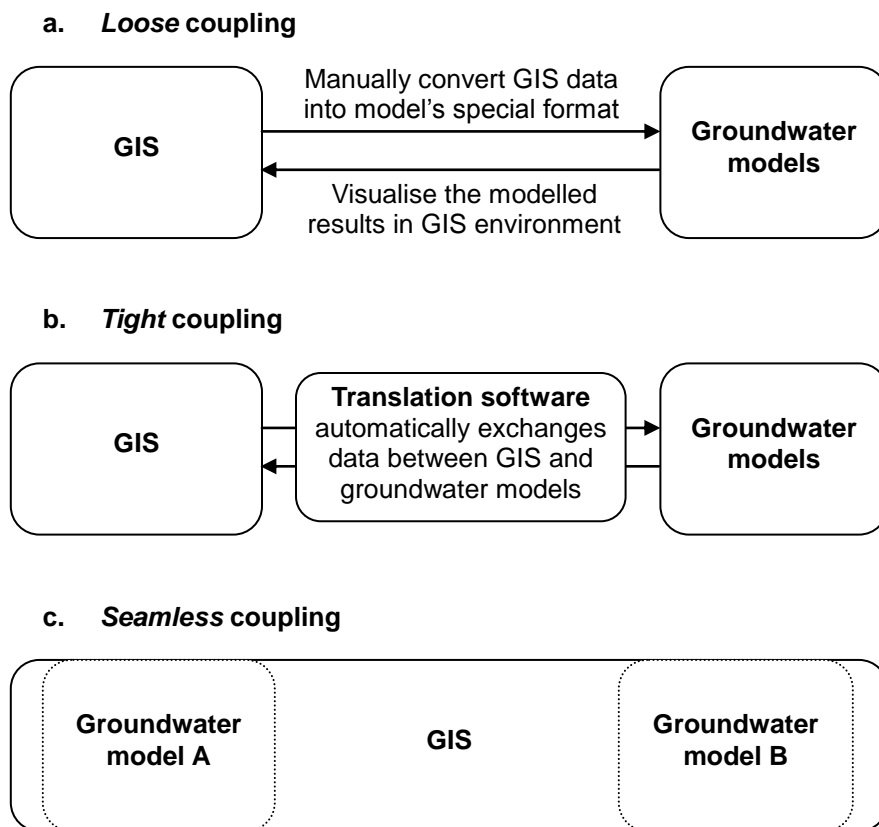
## 30 **1 Introduction**

31 Geographic Information Systems (GISs) are routinely used to process data for input into  
32 complex stand-alone numerical groundwater flow models, such as MODFLOW (Harbaugh  
33 *et al.*, 2000) and FEFLOW (Diersch, 2005). This is because these models require numerous  
34 spatial and temporal datasets that are easily accessed and processed using GIS. Whilst GISs  
35 save users significant time in processing data, in most instances their outputs cannot be  
36 transferred directly into groundwater flow models due to the use of model-specific file  
37 formats. For example the MODFLOW, which is written in the Fortran programming  
38 language, reads text input files using bespoke formats and specific file structures.

39 It has become common practice to couple different numerical models with GISs, and many  
40 efforts have been made to link a GIS and groundwater model using *loose* and *tight* coupling  
41 methods (Bhatt *et al.*, 2014; Vairavamorthy *et al.*, 2007). In *loose* coupling (Fig. 1a) a GIS  
42 is used to manually prepare spatial and temporal datasets for numerical groundwater  
43 models, and to visualise the results generated by them (e.g. Wang *et al.*, 2012, 2013, 2016).  
44 In *tight* coupling (Fig. 1b) computer code is written to automate the exchange of data  
45 between a GIS and a groundwater model, and to translate output from one into the correct  
46 format for the other (e.g. Carrera-Hernández and Gaskin, 2006). The commercial  
47 MODFLOW Analyst code developed in Arc Hydro Groundwater (Strassberg *et al.*, 2011),  
48 which uses the *tight* coupling method, enables users to view, manage and map MODFLOW  
49 models in ArcGIS.

50 In addition to *loose* and *tight* coupling methods, numerical models can be integrated fully  
51 within a GIS using a method referred to as *seamless* coupling (Fig. 1c). Approaches to  
52 *seamless* coupling can be split into two groups. In the first group, groundwater related  
53 models are developed by adopting the existing GIS spatial analysis functions, such as  
54 interpolation, extraction, and raster-layer math (i.e. addition, subtraction, multiplication and  
55 division). Modelling examples listed below belong to this approach: identifying  
56 groundwater recharge zones (Yeh *et al.*, 2009), assessing groundwater pollution  
57 vulnerability (Wang and Yang, 2008; Yang and Wang, 2010) and evaluating groundwater  
58 availability (Ganapuram *et al.*, 2009). In the second group, new models, which use GIS data  
59 format, are developed for GIS from scratch using a computer language (such as C++). The  
60 second group approach makes it possible to develop models representing sophisticated  
61 processes, but complex and time-consuming programming work might be a drawback of  
62 this method. Examples of the second group approach include Arc Hydro (Maidment, 2002)  
63 and the groundwater analysis module in ArcGIS<sup>TM</sup> (ESRI, 2012). The latter was developed  
64 based on the porous medium-advection dispersion model of Tauxe (1994). This ArcGIS<sup>TM</sup>  
65 groundwater module generates a groundwater flow velocity field using groundwater heads.  
66 It is, therefore, actually a post-processing tool for groundwater heads rather than a

67 groundwater flow model that generates groundwater heads. To date there have not been any  
 68 examples of numerical groundwater flow models seamlessly integrated into a GIS for  
 69 producing groundwater heads. Comparing with other coupling methods, the *seamless*  
 70 coupling method makes the groundwater models more efficient and easy-to-use, for the  
 71 processes of data preparation, numerical modelling, post-processing and the visualisation of  
 72 the modelling results are all implemented within a GIS environment. In addition, using the  
 73 standard GIS data formats in *seamless* coupling method means that there is no extra work  
 74 for data exchanging or no extra costs for purchasing coupling interface programs in *tight*  
 75 coupling method (Huang and Jiang, 2002). In this study, we developed a seamless GIS  
 76 groundwater flow model using the second group approach in *Seamless* coupling method.



77

78 Fig. 1 Different methods for coupling groundwater models with GIS.

79 We present a *seamless* GIS-groundwater flow model: BGS GISGroundwater. This model  
 80 uses standard GIS file formats as input and can be regarded as a spatial-analysis tool in  
 81 ArcGIS™. It facilitates the preparation of model input data, simulation of groundwater flow,  
 82 and the visualisation of the modelled results all within a GIS environment.

### 83 2 Model development

84 BGS GISGroundwater is composed of a finite-difference groundwater flow model and a  
 85 User-Interface (UI), which are packaged up as an add-in for ArcGIS™ (Fig. 2). This add-in  
 86 was developed using ArcObjects, a development environment for the ArcGIS™ suite of

87 applications. It generates spatially-distributed groundwater heads by simulating  
 88 groundwater flow in porous media.

### 89 2.1 Numerical groundwater flow model

90 The numerical groundwater flow model solves the governing 2D steady-state groundwater  
 91 flow continuity equation of the form:

92

$$93 \quad \frac{\partial}{\partial x} \left( T_x \frac{\partial h}{\partial x} \right) + \frac{\partial}{\partial y} \left( T_y \frac{\partial h}{\partial y} \right) = Q^A + Q^R - R \quad [1]$$

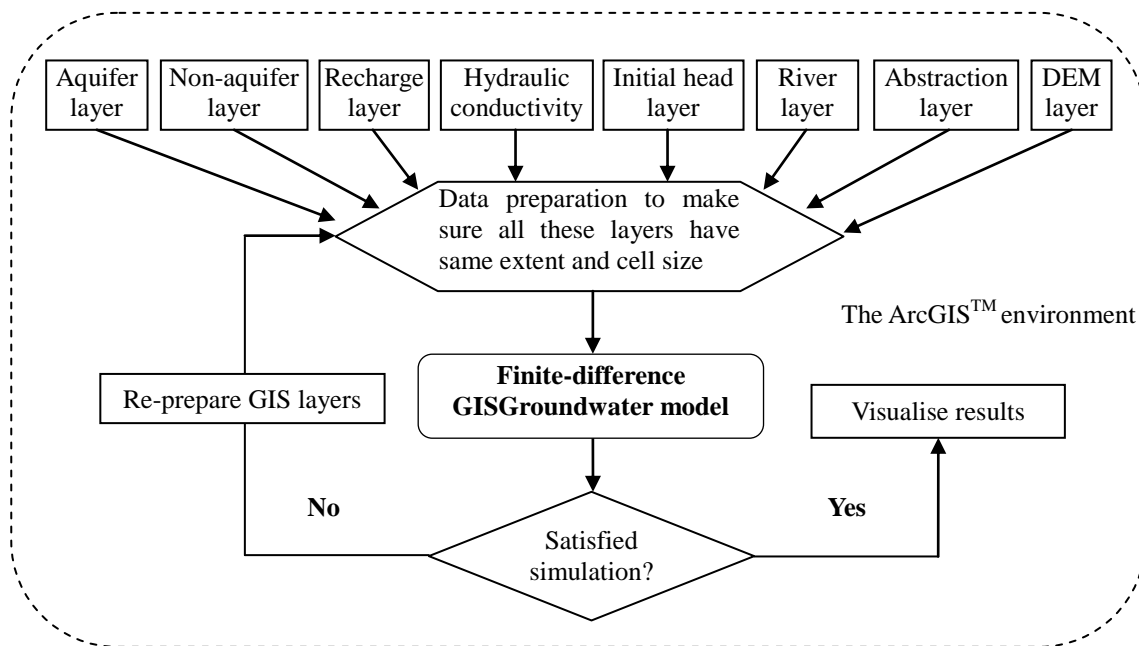
94 where  $h$  is the groundwater head [L];  $T_x$  and  $T_y$  are the aquifer transmissivity in the x and  
 95 y direction respectively [ $L^2 T^{-1}$ ];  $Q^A$  is groundwater abstraction rate [ $L^3 T^{-1}$ ];  $Q^R$  is leakage  
 96 to or from rivers [ $L^3 T^{-1}$ ]; and  $R$  is the amount of groundwater recharge [ $L^3 T^{-1}$ ].

97

98 Whilst equation 1 is the governing equation for aquifers in which transmissivity does not  
 99 vary with saturated thickness, the model can simulate both confined and unconfined  
 100 conditions. To do this the model calculates transmissivity using the hydraulic conductivity,  
 101  $K$  [ $L T^{-1}$ ], as follows:

$$102 \quad T = \begin{cases} K \cdot b & \text{for confined aquifers} \\ K \cdot (h - z_{base}) & \text{for unconfined aquifers} \end{cases} \quad [2]$$

103 where  $b$  is the aquifer thickness [L]; and  $z_{base}$  is the elevation of the aquifer base [L].



104

105 Fig. 2 Structure of BGS GISGroundwater add-in for ArcGIS™.

106

107 Rivers and other surface-water features are represented in the model using a Darcian  
108 head-dependent leakage mechanism, in which inflows and outflows,  $Q^R$ , between the  
109 aquifer and the river, are calculated according to:

$$110 \quad Q^R = C \cdot L \cdot (h - z) \quad [3]$$

111 where  $L$  [L] is the length of the river reach associated with a model cell;  $z$  is the elevation of  
112 surface-water feature [L]; and  $C$  is a leakage coefficient [ $LT^{-1}$ ]. The leakage coefficient  $C$   
113 can be considered to be equivalent to  $K_z w / B$ , where  $w$  is the width of the river, and  $K_z$   
114 and  $B$  are the hydraulic conductivity and thickness of the river bed, respectively.

115 The groundwater model solves Equation 1 for groundwater head using the finite-difference  
116 method (Wang and Anderson, 1982). The aquifer domain is converted into a uniform grid  
117 of cells, at each of which a finite-difference equation is constructed of the form:

$$118 \quad \frac{\left( \frac{T_x^{i,i+1}(h_{i+1,j} - h_{i,j})}{\Delta x_{i+1/2}} - \frac{T_x^{i-1,i}(h_{i,j} - h_{i-1,j})}{\Delta x_{i-1/2}} \right)}{(\Delta x_{i-1/2} + \Delta x_{i+1/2})/2} + \frac{\left( \frac{T_y^{j,j+1}(h_{i,j+1} - h_{i,j})}{\Delta y_{j+1/2}} - \frac{T_y^{j-1,j}(h_{i,j} - h_{i,j-1})}{\Delta y_{j-1/2}} \right)}{(\Delta y_{j-1/2} + \Delta y_{j+1/2})/2}$$

119

$$120 \quad = Q^A + C \cdot L \cdot (h_{i,j} - z) - q \Delta x \Delta y$$

121

$$122 \quad [4]$$

122 where  $i$  and  $j$  are the column and row index of the cell;  $\Delta x_{i-1/2} = x_i - x_{i-1}$ ,  
123  $\Delta y_{j-1/2} = y_j - y_{j-1}$ , and  $T_x^{i-1,i}$  and  $T_y^{j-1,j}$  are the harmonic mean of the transmissivity in  
124 the x and y directions, between cells  $i-1$  and  $i$ , and cells  $j-1$  and  $j$ , respectively; and  $q$   
125 represents groundwater recharge or infiltration from the surface [ $L T^{-1}$ ].

126 The resulting matrix of finite-difference equations for the governing flow equation is solved  
127 using the Point Successive Over-Relaxation (PSOR) method (Wang and Anderson, 1982).  
128 The user defines the maximum number of iterations, a convergence criterion as a maximum  
129 nodal flow imbalance ( $m^3 \text{ day}^{-1}$ ), and the algorithm's over-relaxation parameter,  $\omega$  (Wang  
130 and Anderson, 1982). For unconfined aquifers, the user also defines the number of  
131 transmissivity recalculation cycles to perform.

132 Distributed information on groundwater recharge, abstraction, aquifer hydraulic  
133 conductivity, initial heads and boundary conditions are required for a groundwater flow  
134 solution to be calculated (Fig. 2). Model boundaries are assumed to be no-flow unless  
135 specified as constant head, though flux boundaries can be specified through assignment of  
136 pumping wells.

137 The extent of the model domain, and therefore finite-difference grid, are defined using a  
138 GIS raster layer that maps the area of the aquifer to be modelled. The centre of each raster  
139 cell defines the location of the finite-difference node, and therefore the raster cell edges can  
140 be regarded as forming the *dual mesh* of the finite-difference grid (Fig. 3). We implement a  
141 commonly-used mesh-centred finite-difference grid in which solution nodes are located on

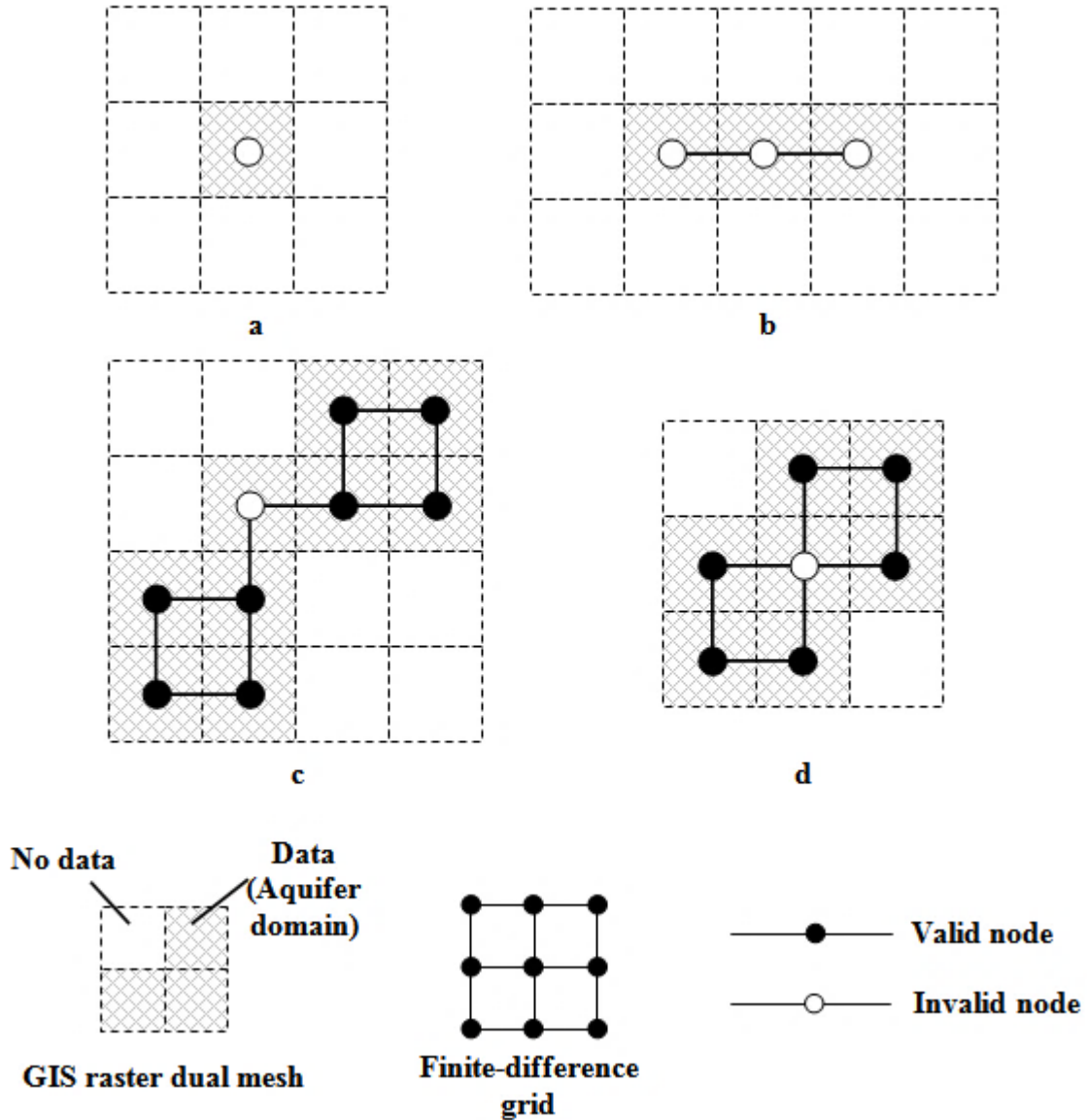
142 no flow (Neumann type) and fixed head (Dirichlet type) aquifer boundaries. This is  
143 different from block-centred finite-difference models in which, a block, or cell, edge  
144 coincides with Neumann boundaries, and the solution node is half a block width inside the  
145 boundary. The model requires at least two lines (i.e. rows and columns) of finite-difference  
146 nodes to be constructed in each Cartesian direction i.e. a single line of finite-difference  
147 nodes is not acceptable. Other problems could arise when converting the aquifer GIS raster  
148 layer into the finite-difference grid in a few specific cases (e.g. Fig. 3). For example, the  
149 invalid node in Fig. 3c is actually located in a non-modelling area in the finite-difference  
150 domain after conversion. In Fig. 3d, the invalid node, which is surrounded by four  
151 boundary nodes, stops groundwater flow in each Cartesian direction within the central dual  
152 mesh. However, these are recognised and automatically removed by the model. The  
153 removal of invalid nodes could create new invalid ones, so this process is iterated until all  
154 nodes in a model are valid. Consequently, the construction of the finite-difference grid for  
155 aquifers with complicated shapes (e.g. Fig. 4) is a straightforward process when using BGS  
156 GISGroundwater.

157

## 158 **2.2 User Interface**

159 The BGS GISGroundwater UI for ArcGIS™ incorporates functions to process model input  
160 data, run a simulation, and visualise the model results. Data preparation functions are  
161 included to enter and check the extent and cell size of GIS data, and to modify data when  
162 necessary to meet the requirements of BGS GISGroundwater. For example, when GIS  
163 raster layers are larger than the extent of aquifer layer, they will automatically be clipped to  
164 the required extent by the interface. If a river shapefile is selected, it will automatically  
165 prepare the river input data by extracting river level values from a Digital Terrain Model  
166 (DTM) layer. The full input data formats for the model are described in Wang *et al.* (2014).

167 Before starting a simulation, the model will check the inputs and highlight any errors. If the  
168 model run is successful the simulated groundwater head layer is displayed in ArcMap™,  
169 along with the modelled area. A message is sent to the user if there are any problems during  
170 the simulation. However, the interface remains open and retains the input data whether  
171 there are errors or not, and subsequently adjusting and re-running a model is straight  
172 forward (Fig. 2).



173

174 Fig. 3 Some examples of GIS grids that create invalid nodes for BGS GISGroundwater.

175

176

177 **3 Model application**

178 BGS GISGroundwater has been validated against analytical solutions to groundwater-head  
 179 profiles, for a range of aquifer configurations. For example, the groundwater-head profile in  
 180 two variants of the aquifer shown in Fig. 5. This 10 km square is represented using a  
 181 uniform, node-centred finite-difference mesh of 500 m-square cells. Recharge is applied  
 182 uniformly across the aquifer at a rate of  $10^{-3}$  m day<sup>-1</sup>. All of the boundaries of the domain  
 183 are specified as impermeable except in the left-hand column of nodes ( $x = 0$ ) where the  
 184 groundwater head is fixed at 100 m. In the first model simulation, transmissivity,  $T$ , is not a  
 185 function of groundwater head and is defined according to the equation:

186

$$T=10\sqrt{x+1000}$$

[5]

187

where  $x$  is the distance in the  $x$  direction from the centre of the left-hand column of fixed-head nodes. The analytical solution of the 1D steady-state groundwater-head profile for this aquifer configuration is:

190

$$h(x) = \frac{q}{5}\sqrt{x+1000}(L-x) + \frac{2q}{15}(x+1000)^{1.5} - \frac{2q}{15}(1000)^{1.5} - \frac{\sqrt{1000}qL}{5} + H_0 \quad [6]$$

191

where  $L$  is the length of the aquifer in the  $x$  direction (10000 m); and  $H_0$  is the fixed-head value on the left-hand boundary.

193

In the second simulation the model is specified to be unconfined, in which case the transmissivity is calculated as the saturated thickness of the aquifer multiplied by the hydraulic conductivity. The aquifer is homogenous with a hydraulic conductivity,  $K$ , of  $10 \text{ m day}^{-1}$  and base elevation,  $z_b$ , of 50 m. For this aquifer configuration, the analytical solution to the steady-state groundwater-head profile is calculated by solving the quadratic equation  $ah^2 + bh + c = 0$  where:

199

$$a = \frac{K}{2}, \quad b = -Kz_b, \quad c = \frac{qx}{2}(x-2L) - \frac{KH_0}{2}(H_0 - 2z_b) \quad [7]$$

200

for selected values of  $x$ .

201

Fig. 6 shows that the results of both models and the analytical solutions are in close agreement. In both simulations the model converges when the maximum nodal flow imbalance at each model cell is less than the specified value of  $10^{-5} \text{ m}^3 \text{ day}^{-1}$ . In the unconfined simulation, 50 transmissivity-recalculation cycles are performed. The maximum differences in groundwater head between the simulated results and analytical solution occur on the right-hand boundary, and are 0.23 m and 0.07 m in the specified-transmissivity and unconfined models, respectively.

208

209

210

211

212

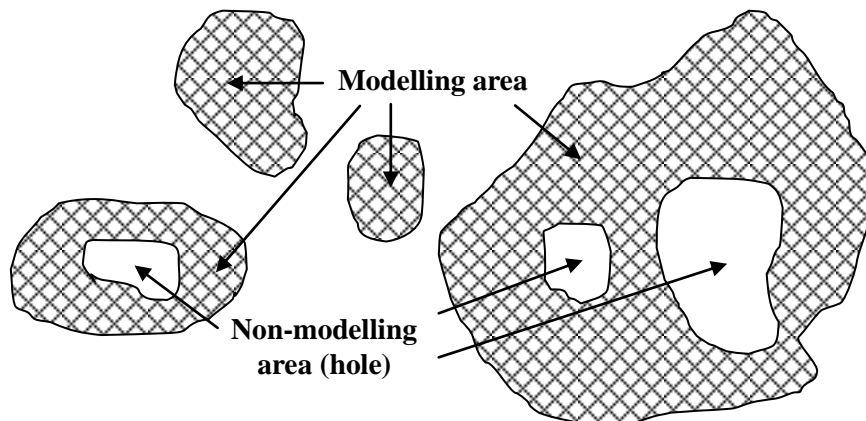
213

214

215

216

217



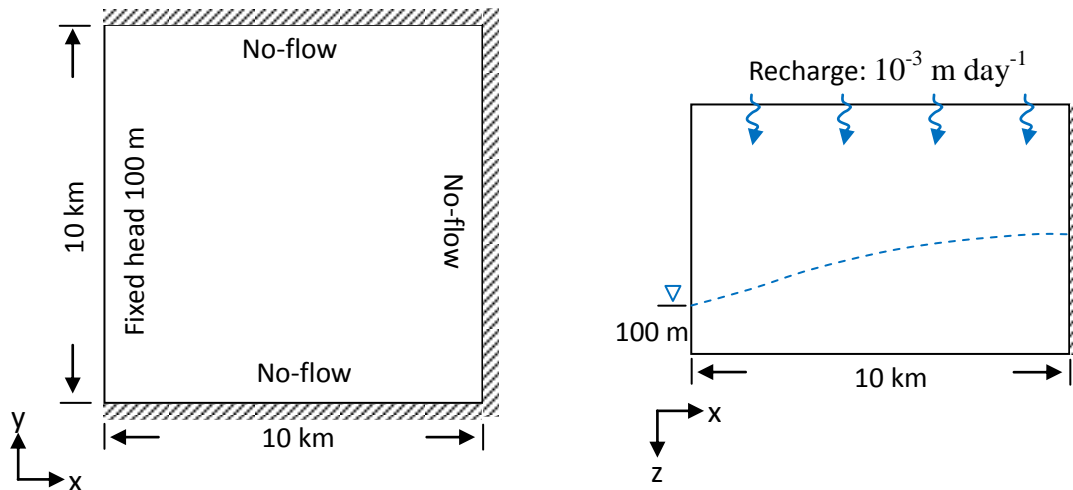
219

Fig. 4 An example of complicated shapes for the modelling extent that BGS GISGroundwater supports.

221

222

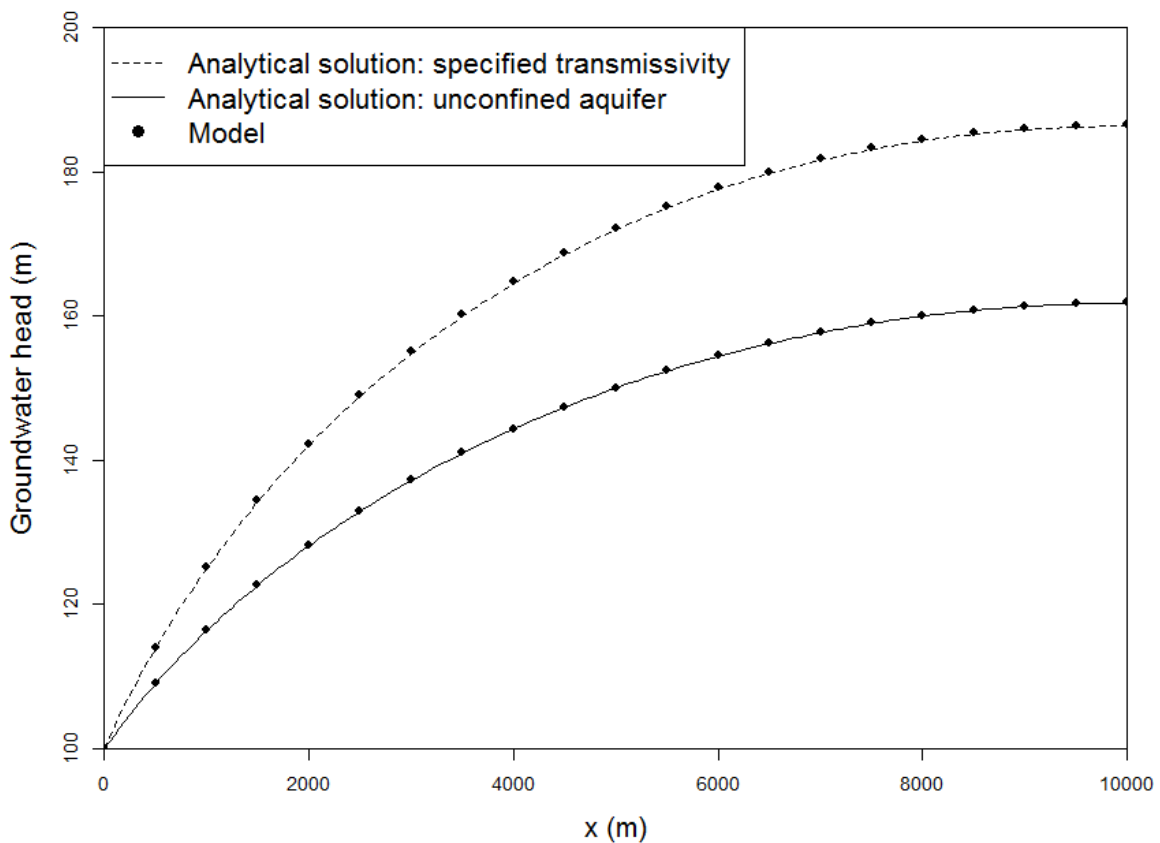




223 Fig. 5 The sketch map of the aquifer for validating BGS GISGroundwater using an analytic  
 224 solution.

225

226



227

228 Fig. 6 The comparison of analytical solutions with the modelled results using BGS  
 229 GISGroundwater.

230

231 **4 Conclusions**

232 BGS GISGroundwater, which is a seamlessly coupled GIS and distributed groundwater  
233 flow model, has been successfully developed, verified and tested in this study. It facilitates  
234 the construction and simulation of the model, and the visualisation of the modelled results  
235 all within the GIS environment. BGS GISGroundwater is relatively simple but can  
236 represent heterogeneous aquifers, variably confined and unconfined conditions, and  
237 distributed groundwater recharge and abstraction. It is an easy-to-use and flexible tool that  
238 lowers barriers to entry to groundwater flow modelling, and enables those with an interest  
239 in understanding aquifers, but with little or no experience in modelling, to develop  
240 groundwater flow models. In addition, the numerical model developed in this study can be  
241 integrated into other GIS packages that support GIS raster data.

242

243 **5 Acknowledgements**

244 The authors gratefully acknowledge the funding provided by core science funds of the  
245 British Geological Survey's Environmental Modelling Directorate, and a Natural  
246 Environment Research Council (NERC) New Investigator grant (NE/K001027/1). The  
247 authors publish with the permission of the Executive Director of the British Geological  
248 Survey (Natural Environment Research Council).

249

250 **References**

- 251 Bhatt, G., Kumar, M., Duffy, C.J., 2014. A tightly coupled GIS and distributed hydrologic  
252 modeling framework. *Environmental Modelling & Software* 62, 70–84.
- 253 Carrera-Hernández, J.J., Gaskin, S.J., 2006. The groundwater modeling tool for GRASS  
254 (GMTG): Open source groundwater flow modeling. *Computers & Geosciences* 32(3),  
255 339–351.
- 256 Diersch, H.J. G., 2005. FEFLOW finite element subsurface flow & transport simulation  
257 system reference manual. Tech. report, WASY GmbH, Berlin, Germany.
- 258 ESRI, 2012. ArcGIS Desktop 10.0 help. [online] URL:  
259 <http://help.arcgis.com/En/Arcgisdesktop/10.0/Help/index.html>.
- 260 Ganapuram, S., Kumar, G.T.V., Krishna, I.V.M., Kahya, E., Demirel, M.C., 2009. Mapping  
261 of groundwater potential zones in the Musi basin using remote sensing data and GIS.  
262 *Advances in Engineering Software* 40(7), 506–518.
- 263 Harbaugh, A., Banta, E., Hill, M., McDonald, M., 2000. MODFLOW-2000, the US  
264 Geological Survey Modular Ground-Water Model – User Guide to Modularization  
265 Concepts and the Ground-Water Flow Process. U.S. Geological Survey.
- 266 Huang, B., Jiang, B., 2002. AVTOP: a full integration of TOPMODEL into GIS,  
267 *Environmental Modelling & Software* 17, 261–268.
- 268 Maidment, D., 2002. Arc Hydro: GIS for Water Resources. Redlands, ESRI Press,  
269 California.
- 270 Strassberg, G., Jones, N.L., Maidment, D.R., 2011. Arc Hydro Groundwater: GIS for

271 hydrogeology. ESRI Press, California.

272 Tauxe, J. D., 1994. Porous Medium Advection–Dispersion Modeling in a Geographic  
273 Information System. Technical Report CRWR 253, University of Texas, Austin.

274 Vairavamoorthy, K., Yan, J, Galgale, H.M and Gorantiwar, S.D., 2007. IRA-WDS- A GIS  
275 based risk analysis tool for water distribution systems, *Environmental Modelling &*  
276 *Software* 22, 951–965.

277 Wang, H.F., Anderson, M.P., 1982. Introduction to groundwater modeling: Finite difference  
278 and finite element methods. Freeman and Co, San Diego, 237 pp.

279 Wang, L., Butcher, A.S., Stuart, M.E., Gooddy, D.C., Bloomfield, J.P., 2013. The nitrate  
280 time bomb: a numerical way to investigate nitrate storage and lag time in the unsaturated  
281 zone. *Environmental Geochemistry and Health* 35 (5), 667-681.

282 Wang, L., Pachocka, M., Jackson, C.R., 2014. User's manual for BGS GISGroundwater: a  
283 numerical model to simulate groundwater levels for ArcGIS. External Report OR/12/063,  
284 British Geological Survey, Keyworth, Nottingham, UK.

285 Wang, L., Stuart, M.E., Bloomfield, J.P., Butcher, A.S., Gooddy D.C., McKenzie, A.A.,  
286 Lewis, M.A., Williams, A.T., 2012. Prediction of the arrival of peak nitrate  
287 concentrations at the water table at the regional scale in Great Britain. *Hydrological*  
288 *Processes* 26, 226–239.

289 Wang, L., Stuart, M.E., Lewis, M.A., Ward, R.S., Skirvin, D., Naden, P.S., Collins, A.L.,  
290 Ascott, M.J., 2016. The changing trend in nitrate concentrations in major aquifers due to  
291 historical nitrate loading from agricultural land across England and Wales from 1925 to  
292 2150. *Science of the Total Environment* 542, 694–705.

293 Wang, L., Yang, Y.S., 2008. An approach for catchment-scale groundwater nitrate risk  
294 assessment from diffuse agricultural sources: a case study in the Upper Bann, Northern  
295 Ireland. *Hydrological Processes* 22, 4274–4286.

296 Yang, Y.S., Wang, L., 2010. Catchment-scale vulnerability assessment of groundwater  
297 pollution from diffuse sources using the DRASTIC method: a case study. *Hydrological*  
298 *Sciences Journal* 55 (7). 1206-1216. 10.1080/02626667.2010.508872.

299 Yeh, H.F., Lee, C.H., Hus, K.C., Chang, P.H., 2009. GIS for the assessment of the  
300 groundwater recharge potential zone. *Environ Geol* 58, 185–195.

301